symmetry

MDPI

Article

Collaborative Spectrum Sensing Algorithm Based on Exponential Entropy in Cognitive Radio Networks

Fang Ye *, Xun Zhang and Yibing Li

College of Information and Communication Engineering, Harbin Engineering University, Harbin 150001, China; zhangxun0611@hrbeu.edu.cn (X.Z.); liyibing0920@126.com (Y.L.)
* Correspondence: yefang0815@126.com; Tel.: +86-131-5980-0815

Academic Editor: Ka Lok Man
Received: 14 June 2016; Accepted: 21 October 2016; Published: 26 October 2016

Abstract: Traditional detectors for spectrum sensing in cognitive radio networks always become disabled when noise uncertainty is severe. Shannon entropy-based detection methods have aroused widespread attention in recent years due to the characteristics of effective anti-noise uncertainty. However, in existing entropy-based sensing schemes, the uniform quantization method cannot guarantee the maximum entropy distribution when primary users do not exist, and cannot effectively distinguish between two hypotheses, which severely limits the promotion of detection performance. Moreover, the Shannon entropy-based sensing schemes are prone to misconvergence occurring when estimating entropy values, thus causing failure detection, which leads to system detection inefficiency and resource waste. These are the two major serious defects in Shannon entropy-based detectors, which restrict the performance improvement. In this paper, a novel non-uniform quantized exponential entropy-based (NQEE) detector is proposed for local sensing to deal with the problems of maximum entropy distribution and detection failure. To further improve the reliability of the detection, a collaborative spectrum sensing algorithm based on an NQEE detector with multiple fusion rules is presented. Simulation results verify that the detection performance of the improved local entropy-based detector is superior to the existing Shannon entropy-based detectors and is proved to be robust to noise power uncertainty. In addition, the novel collaborative detection algorithm outperforms the traditional collaborative spectrum detection method to a great degree.

Keywords: cognitive radio networks; collaborative spectrum sensing; exponential entropy; multi-fusion rule

1. Introduction

With the rapid development of wireless communication business, demand for wireless spectrum resources has grown exponentially in recent years. Given the limitations of natural frequency spectrums, the current fixed radio spectrum allocation policy makes it impossible to satisfy all of the new requirements. Cognitive radio (CR) [1], as a kind of spectrum reutilize technology, can improve utilization efficiency by employing dynamic spectrum allocation (DSA) [2,3]. Secondary users (SUs) are allowed to use the radio spectrum licensed to the primary users (PUs) when the spectrum is temporarily underutilized. In order to support this spectrum reuse functionality, SUs are required to sense the radio frequency environment and vacate the channel instantly without causing any interference once the PUs are found to be active. Therefore, spectrum sensing is of vital importance in cognitive radio networks (CRNs).

Traditional local detection strategies normally adopt matched filter detection [4], energy detection [5] and cyclostationary feature detection [6]. Both matched filter detection and cyclostationary feature detection require certain prior knowledge about the PU signal as well as large computational costs, which are not suitable to act as a blind detector. Energy detection is shown to be optimal when the

cognitive devices do not have prior information about the PU signals, and it possesses low computational costs and is easily implemented. Nevertheless, energy detection is sensitive to noise uncertainty and performs poorly at a low signal-to-noise ratio (SNR). The above traditional detectors are susceptible to noise uncertainty in practical systems, which is a fundamental limitation of current spectrum sensing strategies in detecting the presence of PUs in CRNs. Due to noise uncertainty, the performance of traditional detectors deteriorates rapidly with low SNR.

Fortunately, the entropy-based detectors can effectively overcome the influence of noise uncertainty and improve the robustness of sensing schemes, and hence have obtained extensive research in recent years [7–13]. Dr S. Nagaraj combined the entropy-based detection and matched filter in the time domain in [7,8], but the matched filter needed prior knowledge about PU features, which required additional overhead as a non-blind detector. Zhang et al. proposed a Shannon entropy-based sensing scheme in the frequency domain based on spectrum amplitude (SASE) in [9,10], and the scheme was proved to be robust against noise uncertainty. However, there still exists severe problems such as the maximum entropy distribution in the absence of PUs and detection failure phenomenon. Since an entropy-based detection scheme was proposed, plenty of researchers have conducted comprehensive studies based on Shannon entropy. In [11], a Shannon entropy-based detection scheme based on spectrum power (SPSE) was depicted, the deficiency of which is that computational complexity increases as well as system overhead. In addition, its performance still can be improved. Waleed et al. proposed a robust entropy-based optimization cooperative sensing scheme in [12]; however, the method is only applicable in special occasions, say high sea areas; thus, it does not possess the universality for extensive application. A conditional entropy-based detection method improving the detection performance in low SNR was proposed in [13]. The scheme requires prior information of the system to accurately estimate the unauthorized signal characteristics, which is also a non-blind detection.

In order to enhance sensing performance, more sensing time is needed. However, during the process of sensing, secondary users should stop data transmission to avoid being recognized as primary users. Therefore, more sensing time means lower secondary system capacity, making this approach less attractive. Collaborative spectrum sensing [14–18] (CSS), where local secondary users sense and then send sensing information to the fusion center where the final decision is made, has been studied extensively as a promising alternative to improve sensing performance. There are mainly three schemes of CSS: AND-rule-based CSS [14], OR-rule-based CSS [15], and VOTING-rule-based CSS [16]. However, these CSS schemes are quite simple, and their performance is limited. Recently, the CSS schemes based on weight have been proposed [17,18] with excellent performance; however, in these schemes, SNR of each SU should be estimated perfectly to get the fusion weight, and it is difficult to realize in practical systems.

In this paper, a novel collaborative spectrum sensing (CSS) algorithm based on exponential entropy is proposed. Firstly, in order to solve the problem of the maximum entropy distribution in the absence of PUs, and to avoid detection failure phenomenon in Shannon entropy, a non-uniform quantized exponential entropy-based detection (NQEE) scheme is proposed. To further improve the detection reliability, a novel exponential entropy-based collaborative spectrum sensing scheme with the multi-fusion rule, which adopts an NQEE detector in local sensing, is designed. Local exponential entropy estimation are divided into reliable and unreliable information entropy areas according to the decision area classification rule. SUs transmit one bit or two bits to the fusion center (FC) for decision fusion. The detection performance of the novel scheme is much better than classical CSS schemes. In addition, the scheme is proved to be robust against the noise uncertainty.

The rest of the paper is organized as follows. Section 2 presents the system model for spectrum sensing as well as the defects in previous Shannon entropy-based detectors. In Section 3, we elaborate on the proposed exponential entropy-based CSS scheme, where the NQEE method is applied in local sensing. In Section 4, the NQEE-CSS scheme based on a multi-fusion rule is proposed. Section 5

details performance evaluation and comparisons through plenty of simulations. Finally, conclusions of this paper are drawn in Section 6.

2. System Model and Problem Statement

2.1. System Model

Spectrum sensing can be formularized as a following binary hypothesis problem as follows:

$$x(n) = \begin{cases} w(n), & \mathcal{H}_0 (n = 0, 1, \ldots, N-1), \\ s(n) + w(n), & \mathcal{H}_1 \ (n = 0, 1, \ldots, N-1), \end{cases} \tag{1}$$

where $x(n)$, $s(n)$ and $w(n)$ are, respectively, the received signal, the primary signal and background noise. N is the sample size during the observation period. $\mathcal{H}_0$ / $\mathcal{H}_1$ represent the idle/busy state of channels, respectively. A standard assumption in the literature, which we also make throughout this article, is that the additive noise $w(n)$ is zero-mean, white, and circularly symmetric complex Gaussian (AWGN) with variance σ_n^2. Signal $s(n)$ can either be a deterministic signal (accounting for AWGN channel) or a stochastic signal (corresponding to channel characteristics like fading) with mean μ_s and variance σ_s^2. $s(n)$ and $w(n)$ are mutually independent.

Applying Discrete Fourier Transform (DFT) to (1), we have the frequency domain form of received signal:

$$\vec{X}(k) = \begin{cases} \vec{W}(k), & \mathcal{H}_0 \ (k = 0, 1, \ldots, K-1), \\ \vec{S}(k) + \vec{W}(k), & \mathcal{H}_1 \ (k = 0, 1, \ldots, K-1), \end{cases} \tag{2}$$

where K is the length of DFT equal to sample size N, $\vec{X}(k)$, $\vec{S}(k)$ and $\vec{W}(k)$ are, respectively, the complex spectrum of the receiver signal, primary signal and noise.

The complex spectrum of received signal is expressed as follows:

$$\vec{X}(k) = X_r(k) + jX_i(k) = \frac{1}{N} \sum_{n=0}^{N-1} x(n) \exp(-j\frac{2\pi}{N}kn). \tag{3}$$

Under hypothesis $\mathcal{H}_0$, both the real and imaginary parts of received signal $\vec{X}(k)$ follow the Gaussian distribution $\mathcal{N}(0, \frac{\sigma_0^2}{2N})$, and the spectrum magnitude of follows Rayleigh distribution with parameter $\frac{\sigma_0^2}{2N}$. On the other side, the received signal consists of PU signal and noise under hypothesis $\mathcal{H}_1$, and the spectrum magnitude of $\vec{X}(k)$ follows the Rice distribution. Ascribed to the different probability distributions between Rayleigh distribution and Rice distribution, the detection of the presence/absence of the primary signal can be realized.

Shannon entropy [19] (SE) is used for measuring the size of the average information uncertainty and can be the measurement of ordering degree for systems. The Shannon entropy for a discrete random variable **X** with sample space $[x_1, x_2], [x_2, x_3], \ldots, [x_L, +\infty]$ is

$$H(\mathbf{X}) = E[log_2 \frac{1}{P(x_i)}] = -\sum_{i=1}^{L} P(x_i) \log_2 P(x_i), \tag{4}$$

where L denotes the number of quantized intervals, and $P(x_i)$ is the probability of sample x_i in each interval.

The authors in [9] propose a Shannon entropy-based spectrum sensing scheme in the frequency domain based on the spectrum amplitude, and they proved that the information entropy of the white Gaussian noise (WGN) is a constant with probability space partitioned into fixed dimensions, and the entropy detection based on spectrum amplitude is thus intrinsically robust against noise uncertainty. The decision rule is as follows:

$$H(\mathbf{X}) = -\sum_{i=1}^{L} \frac{n_i}{N} \log_2(\frac{n_i}{N}) \begin{cases} > \lambda, & \mathcal{H}_0, \\ \leqslant \lambda, & \mathcal{H}_1, \end{cases} \tag{5}$$

where n_i represents the numbers of sequence $\mathbf{X}$ falling into ith quantized interval; and λ is the threshold determined by the false alarm probability.

2.2. Problem Statement

Theoretical analysis and simulation in [9] verified the resistance of SASE to noise uncertainty. However, the assumptions and theoretical derivation in the literature have significant limitations, which will be described in detail as follows.

2.2.1. Problem 1—Distribution of the Maximum Entropy under $\mathcal{H}_0$

On the basis of the theory in [9], the uniform quantization Shannon entropy obeys Rayleigh distribution under hypothesis $\mathcal{H}_0$ and deflect Rayleigh distribution under $\mathcal{H}_1$. The authors draw the conclusion that entropy estimation under $\mathcal{H}_0$ is greater than that under $\mathcal{H}_1$. However, it can be known from [19] that Gauss distribution has the maximum differential entropy, and Rayleigh distribution is non-maximum entropy distribution, which means that the conclusion that the entropy of Rayleigh distribution exceeds other distributions is incorrect and controversial. In entropy-based spectrum sensing schemes, if and only if the sample sequence of received signals fall into any quantized interval with then same probability can the maximum entropy distribution then be achieved. As for the detection scheme in [9], the intervals are uniformly divided into fixed dimensions, which cannot ensure equal probability that estimations fall into each range. Hence, the urgent problem to be solved is how to reasonably quantize the probability space and guarantee the maximum entropy distribution in the absence of PUs, meanwhile improving the detection performance to the maximum extent.

2.2.2. Problem 2—The Detection Failure Phenomenon in Shannon Entropy-Based Detectors

The Shannon entropy detection method has certain defects in solving practical problems. According to the definition of Shannon entropy [19], when the probability of detection event x_i is infinitely close to zero, the entropy increment $\Delta I(P_i = 0) = \log_2 \frac{1}{P_i}$ tends to be infinity. Theoretically, for the fixed number of segments L, Shannon entropy estimation X is constant; however, the misconvergence phenomenon $n_i = 0\,(i = 1, 2, \ldots, L)$, $log_2 \frac{n_i}{N} = -\infty$ (n_i represents the signal number falling into ith segment) is prone to occur in practical situations when estimating Shannon entropy, thus causing failure detection, which leads to detection inefficiency and resource waste in the system.

3. Non-Uniform Quantized Exponential Entropy-Based Spectrum (NQEE) Detector

In order to solve the above problems in SASE, we consider using the characteristic that the spectrum amplitude of the received data sequence obeys Rayleigh distribution to detect whether the received signal only contains noise.

3.1. Definition and Property of NQSE

Definition 1. *Given sequential data series,* $\mathbf{X} = \{x_1, \ldots, x_i, \ldots, x_N\}$ *follows the specific distribution* $F_{\mathbf{X}}(x)$*, and non-uniform quantized intervals* $\mathbf{y} = \{y_1, y_2, \ldots, y_L\}$ *are used to conduct L-level quantization for* $\mathbf{X}$*, and the probability of* $\mathbf{X}$ *falling into ith quantized interval is expressed as* p_i*. The non-uniform quantized Shannon entropy of* $\mathbf{X}$ *is*

$$H(\mathbf{X}) = -\sum_{i=1}^{L} p_i \log_2 p_i. \tag{6}$$

The non-uniform quantized Shannon entropy has the following property:

Property 1. *For given sequential data series* $\mathbf{X} = \{x_1, \ldots, x_i, \ldots, x_N\}$ *with specific distribution* $F_{\mathbf{X}}(x)$*, non-uniform quantized intervals* $\mathbf{y} = \{y_1, y_2, \ldots, y_L\}$ *are confirmed by distribution function* $F_{\mathbf{X}}(x)$*, which ensures that* $\mathbf{X}$ *fall into each quantized interval with the same probability* p_i*; thus, the non-uniform quantized entropy achieves the maximum* $\log L$*.*

Proof. According to the Maximum Discrete Shannon Entropy theorem [19]:

$$H(p_1, p_2, \ldots, p_L) \leq H(\frac{1}{L}, \frac{1}{L}, \ldots, \frac{1}{L}) = \log L, \tag{7}$$

where $[p_1, p_2, \ldots, p_L]$ is the distribution law of discrete random variables, and the equality holds up if and only if $p_i = \frac{1}{L}$; that is to say, when the discrete random variable follows the uniform probability distribution, the discrete Shannon entropy reaches the maximum value. Hence, for the specific distribution $F_{\mathbf{X}}(x)$, the maximum entropy $\log L$ is guaranteed to be achieved through determining the non-uniform quantized intervals $\mathbf{y} = \{y_1, y_2, \ldots, y_L\}$, as long as the data sequence falls into each quantized interval with equal probability.

It can be seen from the above property that determining the non-uniform quantized space by Rayleigh distribution can ensure the equal probability of quantized interval $\Delta_k = [y_k, y_{k+1}], (k = 1, 2, \ldots, L)$ and the maximum entropy under hypothesis $\mathcal{H}_0$. □

3.2. Determination of Non-Uniform Quantized Intervals

Assuming random variable V represents event "X falls into quantized intervals", $\{v_1, v_2, \ldots, v_L\}$, respectively, denotes $X(k)$ falling into L quantized intervals. The received signal only contains noise when PU signals does not exist, $X(k)$ falls into L quantized intervals with equal probability and discrete random variable V presents uniform probability distribution. Here, the non-uniform quantization entropy of signal spectrum amplitude can achieve the maximum. On the other hand, when the received signal contains primary signals, random variables V no longer obey uniform probability distribution, and the non-uniform quantized spectrum entropy gets smaller. Cognitive users can determine the presence/absence of PUs according to the difference feature of information entropy measure.

Known amplitude sequence of the received signal obeys the Rayleigh distribution, and the probability distribution function (pdf) of Rayleigh distribution is:

$$F_{\mathbf{X}}(x) = \int_0^{\infty} \frac{x}{\sigma^2} \exp(-\frac{x}{2\sigma^2}) dx = 1 - \exp(-\frac{x}{2\sigma^2}). \tag{8}$$

In order to obtain the uniform probability distribution, combine Equation (8) with the following formula

$$F_{\mathbf{X}}(x_i) = \frac{1}{L}(i-1). \tag{9}$$

Then, the separating points of non-uniform quantized intervals can be obtained by the following expression:

$$x_i = \sqrt{-2\ln(1 - \frac{i-1}{L})}\sigma, \; i = 0, 1, \ldots, N-1. \tag{10}$$

For instance, when the value of L is 10, subsections of Rayleigh distribution, as shown in Figure 1, can be acquired through the process of non-uniform quantization. The x-axis shows the amplitude of the signal in the frequency domain, while the y-axis represents the probability density function of Rayleigh distribution. The probability of received data falling into certain intervals is the area of that interval. It can be qualitatively seen that sequence x falls into ten subsections (1–10) with equal probability.

The noise variance is indispensable for dividing quantization intervals; thus, when the estimation of noise variance is inaccurate or noise fluctuates over time, the process of non-uniform quantization interval will be affected. Taking the above issues into account, we perform normalization processing for

received information sequence $s(k)$ $(k = 0, 1, \ldots, N-1)$, making the Rayleigh distribution parameter σ^2 as 1, and then the influence of the noise uncertainty can be overcome. The quantization interval boundary can be rewritten as

$$x_i = \sqrt{-2\ln(1 - \frac{i-1}{L})},\ i = 0, 1, \ldots, N-1. \tag{11}$$

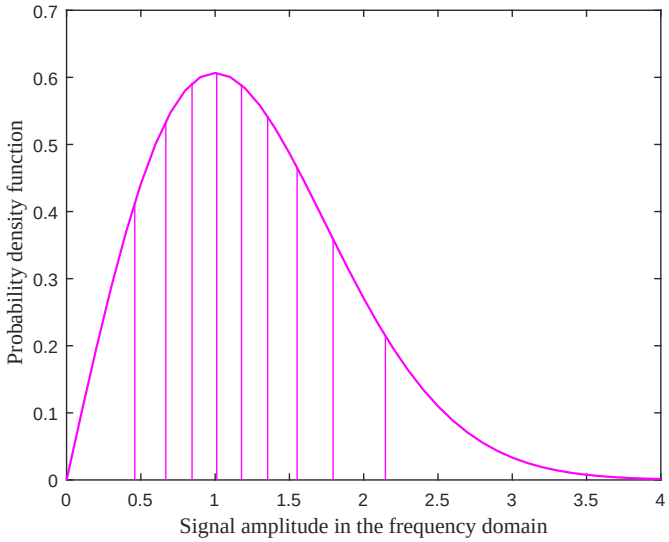

Figure 1. Sketch map for non-uniform quantization under Rayleigh distribution.

3.3. Spectrum Sensing Based on NQSE

Based on the above discussions and analyses, we make the following statements about the implementation process of the non-uniform quantized Shannon entropy-based (NQSE) detection algorithm. Firstly, secondary users perform N-point samples to received signals to obtain the sampling sequence $\mathbf{s} = [s(0), s(1), \ldots, s(N)]$; then, normalization for received sequences $s(k)$ $(k = 0, 1, \ldots, N-1)$ are conducted to get the normalized sequences $s_N(k)$, and the power of received signal sequences become $s_N(k) = \frac{s(k)}{\sqrt{\sum_{i=1}^{N-1}|s(k)|^2}}$; afterwards, DFT is used to obtain spectrum sequences $S(k) = \sum_{l=0}^{N-1} s_N(l)\exp(-j\frac{2\pi}{N}kn)$, and the amplitude of spectrum is $X(k) = S(k)S^*(k)$; subsequently, calculating the quantization intervals $[x_1, x_2], [x_2, x_3], \ldots, [x_L, +\infty]$ according to (11), and counting numbers of the sequence $\mathbf{X} = [X(0), X(1), \ldots, X(N)]$ dropping into each interval, denoted by $[n_1, n_2, \ldots, n_L]$; thus, the non-uniform quantized Shannon entropy (NQSE) of spectrum sequence is

$$H_{SHAN}(\mathbf{X}) = -\sum_{i=1}^{L} \frac{n_i}{N} \log_2(\frac{n_i}{N}). \tag{12}$$

Finally, compare $H_{SHAN}(\mathbf{X})$ with threshold λ. If test statistic $H_{SHAN}(\mathbf{X}) > \lambda$, the authorised channel is judged as free; otherwise, the channel is occupied.

3.4. Spectrum Sensing Based on NQEE

Hereinbefore, we solve the **Problem 1** through the proposal of NQSE. In order to overcome the defect of failure detection problem in SASE, the concept of exponential entropy is introduced into the sensing algorithm. The increment of exponential entropy ΔI is zero when probability $P_i = 0$, and the phenomenon of misconvergence is effectively avoided in the process of estimating entropy. Thus, the problem of failure detection is definitely solved.

The exponential entropy is defined based on the following principles [20]:

(1) Supposing the probability of each state x_i is P_i, then the information content $\Delta I(P_i)$ carried by x_i has definition in all points between $[0, 1]$;
(2) $\lim_{P_i \to 0} \Delta I(P_i) = \Delta I(P_i = 0) = k_1$, k_1 is limited and greater than or equal to 0;
(3) $\Delta I(P_i = 1) = k_2$, k_2 is limited and greater than or equal to 0;
(4) $k_2 < k_1$;
(5) $\Delta I(P_i)$ decreases in exponential form with P_i increasing;
(6) Information content $\Delta I(P_i)$ and entropy H are consecutive between $[0, 1]$;
(7) Entropy H reaches the maximum when $P_i (i = 1, 2, \cdots, L)$ are all equal, i.e., uniform probability distribution.

The exponential entropy which satisfies all principles above is defined as [20]:

$$H_{EXP}(\mathbf{X}) = -\sum_{i=1}^{L} P_i e^{(1-P_i)}. \tag{13}$$

The specific algorithm procedures of non-uniform quantized exponential entropy-based detection are shown in Algorithm 1, and the only difference between the non-uniform quantized exponential entropy-based detection and NQSE is the calculation method of entropy. Exponential entropy has similar properties to Shannon entropy; for instance, exponential entropy is not affected by noise power. In fact, exponential entropy also has no relationship with noise power. That is to say, the NQEE algorithm also possess robustness to the noise power uncertainty. This property will be attested in the following simulation work. By comparing the exponential entropy calculated in Equation (14) with the threshold, the existence of PU signal can be determined. The decision rule can be expressed as

$$H_{EXP}(\mathbf{X}) = -\sum_{i=1}^{L} \frac{n_i}{N} \exp(1 - \frac{n_i}{N}) \begin{cases} > \lambda, & \mathcal{H}_0, \\ \leqslant \lambda, & \mathcal{H}_1. \end{cases} \tag{14}$$

Algorithm 1 Non-uniform Quantized Exponential Entropy-based Detection (NQEE) Algorithm

Input: $\lambda \in \mathbb{R}^+$, $N \in \mathbb{N}$, $L \in \mathbb{N}$.
Output: $S_i \in \{\mathcal{H}_0, \mathcal{H}_1\}$.

for each sensing event **do**
$\mathbf{s} = [s(0), s(1), \ldots, s(N)] \leftarrow$ N-point sampling
$s_N(k) \leftarrow$ perform normalization to s
$\mathbf{X} \leftarrow$ perform Discrete Fourier Transform for s_N
$[x_1, x_2], [x_2, x_3], \ldots, [x_L, +\infty]$ quantized intervals
    for $i = 1, 2, \ldots, L$
        $[n_1, n_2, \ldots, n_L]$ count numbers of each interval
    end for
    $H_{EXP}(\mathbf{X}) = -\sum_{i=1}^{L} \frac{n_i}{N} \exp(1 - \frac{n_i}{N})$
    if $H_{EXP}(\mathbf{X}) > \lambda$ **then**
        $S_i \leftarrow \mathcal{H}_0$
    else
        $S_i \leftarrow \mathcal{H}_1$
    end if
end for

The introduction of exponential entropy effectively evades the problem of no definition or zero value of using logarithms to define entropy and also overcoming the deficiency of the Shannon entropy. The problem of failure detection discussed above has been solved skillfully by introducing the exponential entropy into the spectrum detection algorithm.

4. Collaborative Spectrum Sensing Based On Exponential Entropy

4.1. Traditional CSS Schemes

We consider a CR network consisting of K SUs and a data fusion center (FC). Assume that each CR performs spectrum sensing independently and then their local decisions are sent to the FC, which can fuse all available decision information to infer the presence or absence of the PU.

In traditional "k-out-of-n" rule CSS, each collaborative partner makes a binary decision based on its local observation and then forwards one bit of the decision D_i ($i = 1$ standing for the presence of the PU, $i = 0$ for the absence of the PU) to the FC through an error-free channel. At the FC, all one-bit decisions are fused together according to the logic rule where $\mathcal{H}_0$ and $\mathcal{H}_1$ denote the decision made by the fusion center that the PU signal is transmitted or not, respectively. The threshold k is an integer representing the "k-out-of-n" rule. It can be seen that the OR rule corresponds to the case of $k = 1$, AND rule corresponds to the case of $k = n$, and in the VOTING rule k is equal to the minimal integer larger than $\frac{n}{2}$.

4.2. CSS Based On Exponential Entropy

When SNR becomes lower, the gap between the exponential entropies calculated in the two hypotheses are getting smaller, hence the detection results become trustless. To further improve the performance of the non-uniform quantized exponential entropy detection at low SNR, a novel exponential entropy CSS scheme based on multi-fusion rule (NQEE-CSS) is proposed, which improves the detection performance by farthest use all SUs local sensing results.

In the proposed CSS scheme, the local estimated entropy results in information made by each secondary user being classified into two types, as shown in Figure 2. When estimated entropy satisfies $H(\mathbf{Y}) \leqslant \lambda - \Delta$ or $H(\mathbf{Y}) > \lambda + \Delta$ (Δ is any positive real number, λ is decision threshold), we define this area as reliable information entropy area; otherwise, when entropy is in $\lambda - \Delta < H(\mathbf{Y}) \leqslant \lambda + \Delta$, the area is defined as an unreliable information entropy area. The OR rule is adopted to fuse reliable information entropy, if there is at least one decision result of cognitive user being one, then the fusion result of this region is one. The AND rule is used to merge under-reliable information entropy together, if and only if all decisions of SUs are one, and the final fusion result in the area is one.

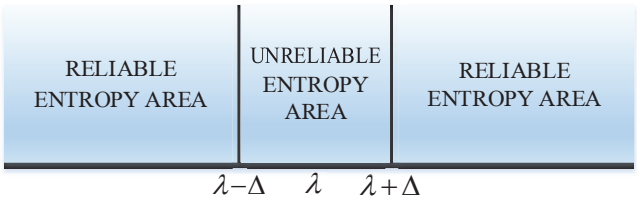

Figure 2. Local decision zoning map.

The process of novel CSS algorithm is shown in Figure 3, and the specific implementation steps are as follows:

Step 1 Each SU conducts independent local sensing. At the ith secondary user, the normalized process for received signal sequences is firstly performed, then the N-point DFT is applied to obtain the spectrum of the received signal $Y(k), k = 1, 2, \ldots, N$. Calculate non-uniform quantized exponential entropy $H(\mathbf{Y})$ of spectrum sequences $\mathbf{Y}$ according to Equation (15).

Step 2 SUs make decisions based on the decision rules as shown in Figure 4. When exponential entropy is in the reliable information area, SUs use one bit to code decision information; otherwise, when entropy is in the under-reliable information area, they adopt two bits to code decisions. Two kinds of decision information obtained by cognitive users are shown below.

One-bit information:

$$D_{1i} = \begin{cases} 0, & H(\mathbf{Y}) \geq \lambda + \Delta, \\ 1, & H(\mathbf{Y}) \leq \lambda - \Delta, \end{cases} \tag{15}$$

Two-bit information:

$$D_{2i} = \begin{cases} 10, & \lambda < H(\mathbf{Y}) < \lambda + \Delta, \\ 11, & \lambda - \Delta < H(\mathbf{Y}) \leq \lambda, \end{cases} \tag{16}$$

where the first bit is the identification information, which represents the estimation entropy falling into the unreliable information entropy area. The second bit is the decision information.

Step 3 All SUs send decision information to the FC. The fusion center receives two types of information: one-bit and two-bit information. The FC extracts the corresponding decision information Z_i from two-bit information:

$$Z_i = \begin{cases} 0, & \lambda < H(\mathbf{Y}) < \lambda + \Delta, \\ 1, & \lambda - \Delta < H(\mathbf{Y}) \leq \lambda. \end{cases} \tag{17}$$

Step 4 Assume that M SUs are involved in collaborative sensing, where K users send one-bit messages, and $M - K$ users send two-bit messages. The FC fuses all messages in light of the difference of information type: OR rule for one-bit messages and AND rule for 2-bit messages. FC makes the final OR rule for the two sorts of results above. The global decision result is as follows:

$$F = \begin{cases} 0, & \sum_{i=1}^{K} D_{1i} + \prod_{i=K+1}^{M} Z_i \geq 1, \\ 1, & \text{else}, \end{cases} \tag{18}$$

where $F = 1$ and $F = 0$, respectively, denote the presence and absence of the PU signal.

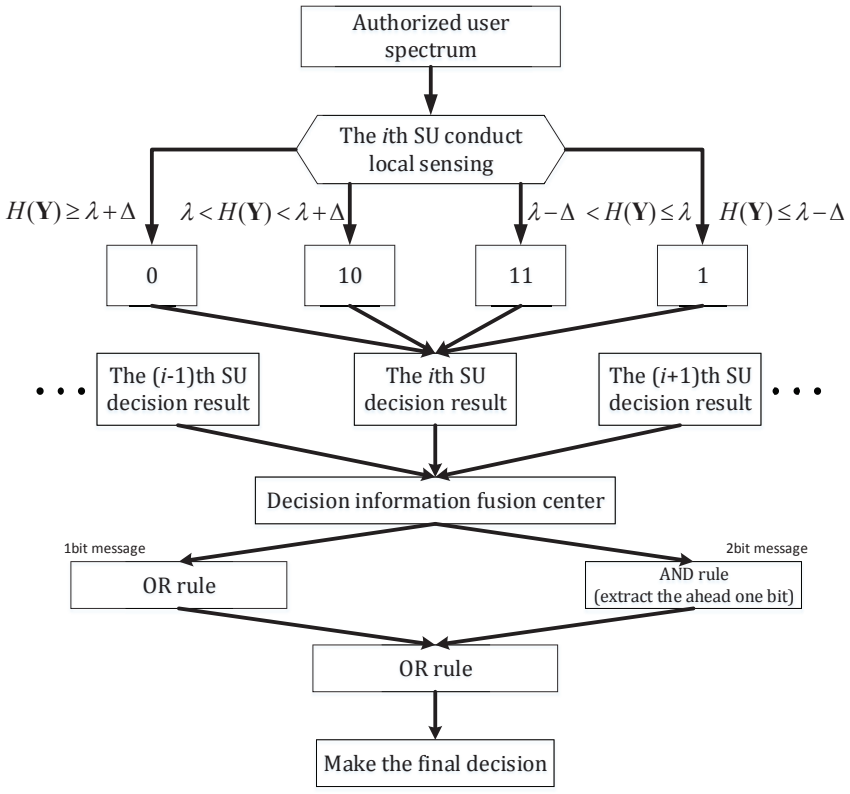

Figure 3. The flow chart of NQEE-CSS algorithm with the multi-fusion rule.

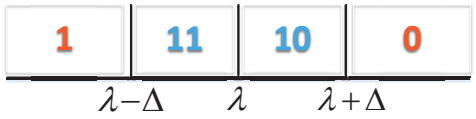

Figure 4. Multi-fusion rule decision area encoding rules.

5. Simulation Results and Analysis

The verification test of detection failure for Shannon entropy is presented in Figure 5. The experiments are divided into three groups, and each group conducts 50 sub-experiments with detection for 100 times. The received signal is AWGN with length $N = 512$ and the bin number L in each experiment is 12, 16, 20, respectively. The abscissa is set as the experiment times and the ordinate is the times of failure detection. It can be seen that there exist different levels of detection failure phenomenon. The proportion of failure obviously rises with L increasing, which can be ascribed to fact that the width of the interval decreases when L increases; therefore, the probability of detection statistics falling into the $i\Delta$th interval becomes higher. When $L = 20$, the average rate of failure detection reaches above 50%. To a large extent, high ratio of detection failure causes low detection efficiency and waste of system resources.

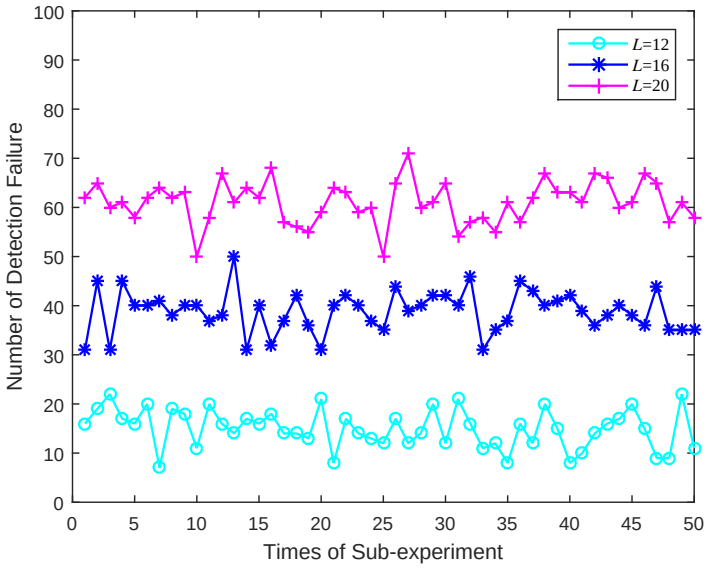

Figure 5. Failure detection experiment for Shannon spectrum entropy.

To evaluate the detection performance of the proposed detection scheme, plenty of simulations are carried out. The signal of the primary user is modulated BPSK signal, baseband symbol rate $R_b = 8$ kbps and carrier frequency $f_c = 16$ kHz. The sampling frequency at the cognitive receiver is set as $f_s = 64$ kHz. The number of non-uniform quantizing interval L of the probability space is 20. The number of Monte Carlo simulation times is 10,000. In all of the entropy-based detectors, the sample size of DFT is equal to 1024 points. The sample size is also equal to 1024 points in energy detection.

In Figure 6, we compare the detection probability of proposed non-uniform quantized exponential entropy-based detection with entropy-based scheme based on power spectral, Shannon entropy-based detection and energy detection. False alarm probability P_f is 0.1, the variation range of SNR is $[-16$ dB, -4 dB$]$ with step length 1 dB. Simulation experiments are under the conditions of the additive white Gaussian noise (AWGN) channel. Overall, the detection performance of the proposed scheme is better than several other solutions. Among which, the NQEE detection conducts non-uniform quantization for probability space according to the characteristics of the spectrum obeying Rayleigh

distribution, which ensures that the entropy estimation achieves the maximum, thus its performance is superior to other detection schemes. In addition, the NQEE spectrum detection scheme overcomes the detection failure problem of Shannon entropy on the basis of NQSE, and its detection performance is apparently superior to the NQSE algorithm. In particular, when detection probability P_d is equal to 0.9, the SNR of the NQEE is about -10 dB, realizing a performance improvement effect of about 2 dB when compared with SASE of -8 dB.

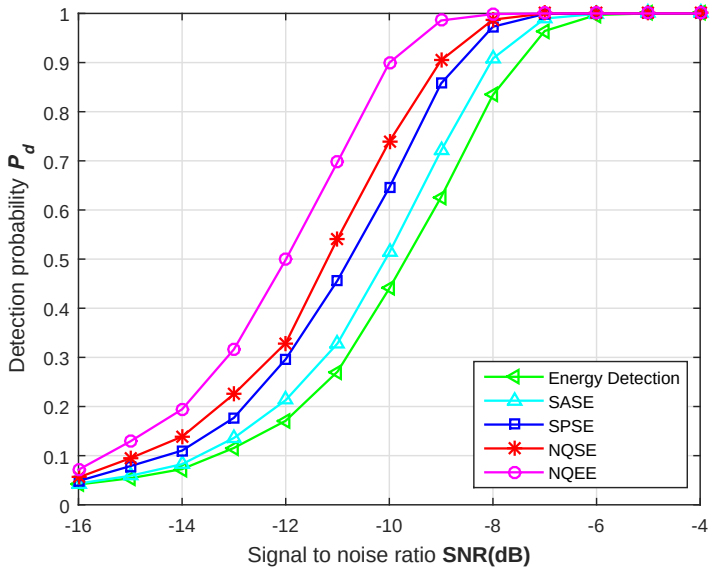

Figure 6. Detection performance against SNR comparison of the detectors.

When SNR is equal to -10 dB, the simulation about the relationship between detection probability P_d and false alarm probability P_f is carried out and the receiver operating characteristics (ROC) curves are shown in Figure 7. Obviously, the NQEE scheme has the best detection performance. Considering $P_f = 0.1$, detection probability of NQEE and SASE are 0.9357 and 0.6960, respectively; thus, the performance promotion of NQEE is roughly 0.24. When P_f is greater than 0.3, the detection probability of four kinds of entropy-based schemes are all greater than 0.9, but, in general, we do not care much about the detection performance under high false alarm probability. Due to the standard of the IEEE 802.22 working group, a false-alarm probability less than or equal to 0.1 is the most conducive for full use of valuable spectrum resources. Hence, the detection performance under low false alarm probability should mainly be considered.

The above simulation and analysis verify that NQEE outperforms similar entropy detection schemes. Besides detection performance, the robustness against noise uncertainty is also presented as a significant measure factor in sensing schemes. While energy detection is very sensitive to the variation of the background noise. Based on this, the simulation concerning the detection performance of NQEE and energy detection under noise uncertainty is conducted in Figure 8. The change range of background noise power in the experiment is $[-98$ dBm, -93 dBm$]$, and SNR is set as -12 dB.

In Figure 8, P_f and P_d of the exponential entropy-based detection remain unchanged with the noise power varying, respectively remaining at 0.6825 and 0.1, which indicates that noise uncertainty cannot affect the performance of the novel entropy-based scheme, and the noise power is -95.5 dBm when P_f of the energy detection and the NQEE detection are both equal to 0.1. The energy detector is extremely sensitive to the noise power uncertainty, and P_f and P_d become unsatisfactory with the noise uncertainty larger than only 0.5 dBm. Thus, the energy detection with a fixed threshold is hardly applicable to actual networks due to the background noise fluctuating in almost all of the practical communication systems.

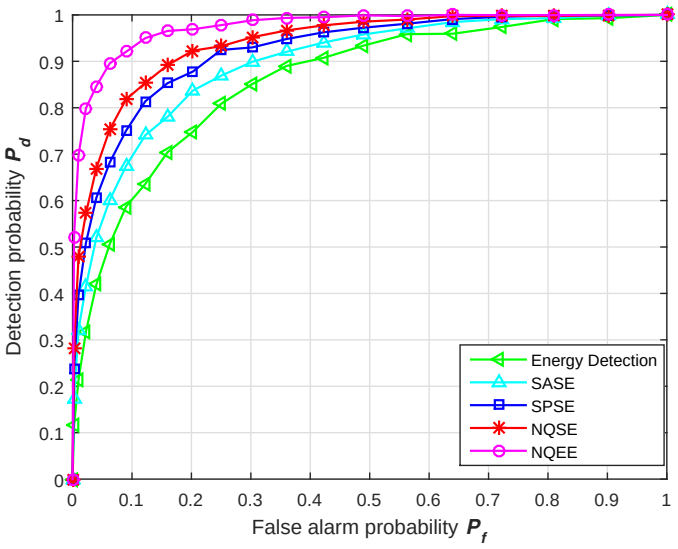

Figure 7. ROC curves comparison of the detectors when SNR is equal to −10 dB.

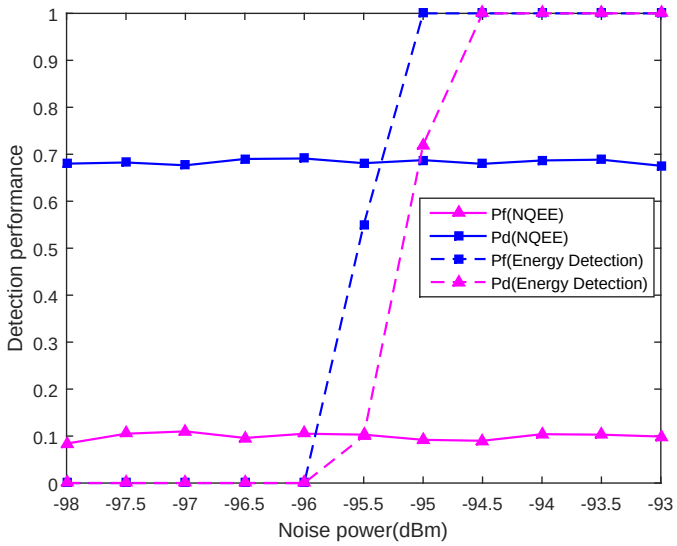

Figure 8. The relationship between detection performance and noise power uncertainty when SNR = −12 dB.

Under the condition that primary signals exist in the authorized spectrum, the simulation about the relationship between exponential entropy and SNR is shown in Figure 9. Sampling numbers are $N1 = 512$, $N2 = 1024$, interval numbers are $L1 = 12$, $L2 = 16$, and $L3 = 20$, and the changing range of SNR is $[-16$ dB, -6 dB$]$. It can be seen that the exponential entropy estimation gets smaller with the increase of SNR. After confirming the decision threshold, detection probability has obvious improvement as SNR increases. On the other hand, it can be derived through the comparisons of three curves that exponential entropy estimation reduces with the reduction of L, thus reducing section numbers is also considered as feasible way to improve detection probability under low SNR. In addition, the sampling number also influences the change of entropy estimation. In this experiment, the entropy estimate index decreases with the increase of sampling points, and detection probability increases with the increase of sampling points. In the case of high SNR, the effect that sampling points exert on exponential entropy estimation weakens.

Δ is a significant parameter in an exponential entropy-based CSS scheme, and the setting of its value should be carefully considered. As shown in Figure 10, we study the relationship between SNR and detection probability P_d: false alarm probability $P_f = 0.1$ and SNR changes from -12 dB to -4 dB. Parameter Δ is, respectively, set as $0.1, 0.2, 0.3, and\ 0.4$. Sample number is 1024, and the number of SUs involved in the CSS M is equal to five. The simulation of exponential entropy-based detection, power spectral entropy-based detection, and energy detection are also shown as contrast curves in the picture. For the fixed SNR, when Δ increases, the detection probability P_d also increases. The reason for this phenomenon is that the probability of exponential entropy estimation information falling into $[\lambda + \Delta, \lambda - \Delta]$ gets larger with the increase of Δ; therefore, the performance of the NQEE-CSS scheme presents an obvious increase. When $\Delta > 2$, the growth rate of detection performance is very small, almost remaining the same. In addition, as mentioned earlier, the detection performance of exponential entropy-based detection method is superior to the power spectrum entropy detection and the energy detection algorithm.

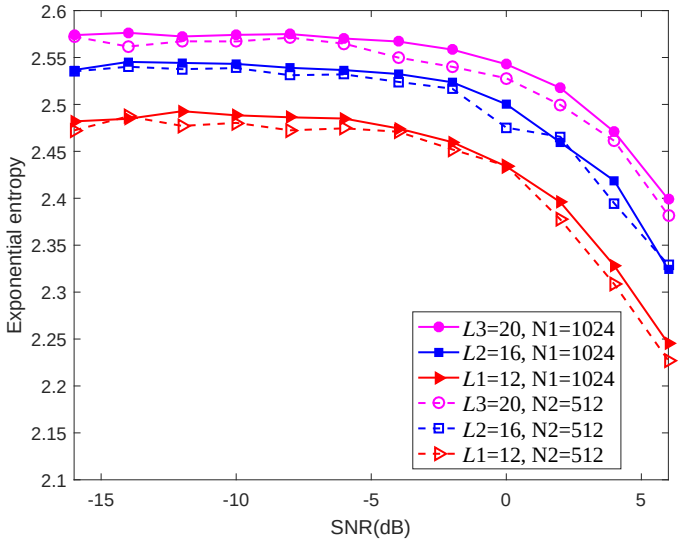

Figure 9. The relationship between exponential entropy and SNR.

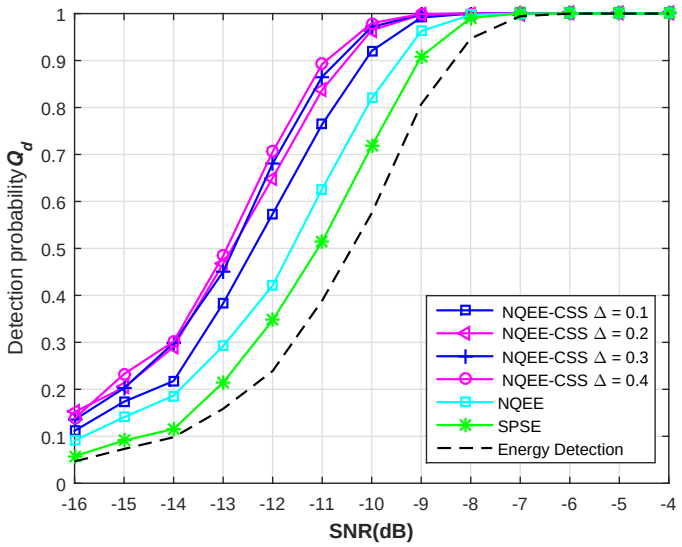

Figure 10. Performance of CSS schemes for different Δ.

We demonstrate the detection performance of proposed exponential entropy CSS algorithm in Figures 11 and 12. In Figure 11, the SNR range is set as $[-16$ dB, -4 dB$]$, P_f is 0.1, $N = 1024$, parameter Δ is 0.2, and simulation is under the channel of AWGN. The performance of exponential entropy-based detection and power spectral entropy detection with a single secondary user is also analyzed. From the simulation results in Figure 11, we can see that the P_d performance of the NQEE-CSS method is much better than the other three traditional cooperative entropy-based detection schemes (AND, OR, and VOTING rules). Especially when SNR is equal to -12dB, the proposed algorithm possesses the 0.162, 0.278 and 0.394 promotion of detection probability, compared with three kinds of traditional collaborative detection methods (based on the exponential entropy), which proves that the proposed CSS algorithm has the superior detection performance with low SNR and is suitable for the actual wireless environment.

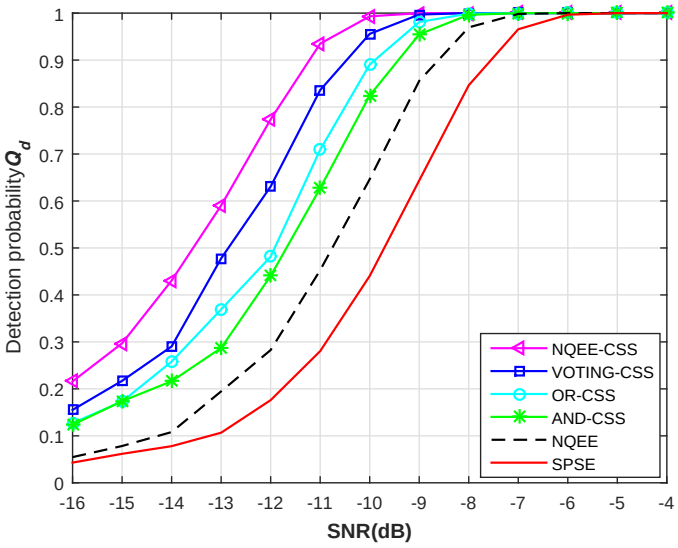

Figure 11. Detection performance against SNR comparison of the entropy-based collaborative detectors.

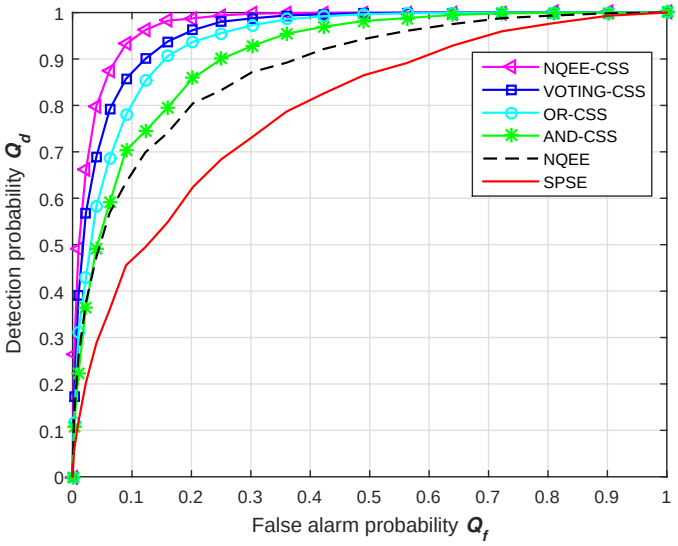

Figure 12. ROC curve comparison of the entropy-based cooperative detectors.

The ROC performances of these entropy-based collaborative detectors are also analyzed and the corresponding ROC curves are depicted in Figure 12. The parameters of these detectors are

the same as those set in Figure 7. From the simulation results in Figure 12, we can see that the ROC performance of the cooperative exponential entropy-based detection scheme is obviously much better than that of the other detectors, especially under the condition of low false alarm probability. When $P_f = 0.1$, the detection probability of exponential entropy CSS achieves 0.534 promotion to the VOTING-CSS scheme.

6. Conclusions

In order to avoid detection failure phenomenon of Shannon entropy and tackle the problem of the maximum entropy distribution in the absence of PUs, a novel exponential entropy-based cooperative spectrum sensing scheme with a multi-fusion rule is designed in this paper. Local exponential entropy-based estimations are divided into reliable and unreliable information entropy areas according to the decision area classification rule. SUs transmit one bit or two bits to the fusion center for the multi-fusion rule. The new cooperative scheme is proved to achieve much better performance than AND, OR, and VOTING rule CSS schemes. Moreover, the scheme is robust against the noise uncertainty.

Acknowledgments: This paper is funded by the National Natural Science Foundation of China (Grant No. 51509049), the Natural Science Foundation of Heilongjiang Province, China (Grant No. F201345), the Fundamental Research Funds for the Central Universities of China (Grant No. GK2080260140), the National Key Foundation for Exploring Scientific Instruments of China (Grant No. 2016YFF0102806).

Author Contributions: Fang Ye conceived the concept and performed the research, Xun Zhang conducted experiments to evaluate the performance of the proposed algorithm and wrote the manuscript, Yibing Li reviewed the manuscript. All authors have read and approved the final manuscript.

Conflicts of Interest: The authors declare no conflict of interest.

References

1. Mitola, J.; Maguire, G.Q. Cognitive radio: Making software radios more personal. *IEEE Pers. Commun.* **1999**, *6*, 13–18.
2. Haykin, S. Cognitive radio: Brain-empowered wireless communications. *IEEE J. Sel. Areas Commun.* **2005**, *23*, 201–220.
3. Li, Y.B.; Yang, R.; Ye, F.; Gao, Z. Improved spectrum sharing algorithm based on feedback control information in cognitive radio networks. *J. Syst. Eng. Electron.* **2013**, *24*, 564–570.
4. Ma, J; Zhao, G; Li, Y. Soft Combination and Detection for Cooperative Spectrum Sensing in Cognitive Radio Networks. *IEEE Trans. Wirel. Commun.* **2008**, *7*, 4502–4507.
5. Digham, F.F.; Alouini, M.S.; Simon, M.K. On the Energy Detection of Unknown Signals over Fading Channels. *IEEE Trans. Commun.* **2007**, *55*, 21–24.
6. Yang, M.; Li, Y.; Liu, X.; Tang, W. Cyclostationary feature detection based spectrum sensing algorithm under complicated electromagnetic environment in cognitive radio networks. *China Commun.* **2015**, *12*, 35–44.
7. Chen, X.; Nagaraj, S. Entropy based spectrum sensing in cognitive radio. In Proceedings of the Wireless Telecommunications Symposium (WTS), Pomona, CA, USA, 24–26 April 2008; pp. 57–61.
8. Nagaraj, S.V. Entropy-based spectrum sensing in cognitive radio. *Signal Process.* **2009**, *89*, 174–180.
9. Zhang, Y. Entropy-based robust spectrum sensing in cognitive radio. *IET Commun.* **2010**, *4*, 428–436.
10. Zhang, Y.L.; Zhang, Q.Y.; Melodia, T. Entropy-based robust spectrum sensing in cognitive radio. *IEEE Commun. Lett.* **2010**, *14*, 533–535.
11. Gao, Y.; Hu, G.B.; Zhang, Z.F.; Jin, M.; Tang, Y. Power Spectral Entropy Based Spectrum Sensing in Cognitive Radio. *Chin. J. Electron Dev.* **2015**, *38*, 506–509.
12. Ejaz, W.; Shah, G.A.; Hasan, N.; Kim, H.S. Optimal Entropy-Based Cooperative Spectrum Sensing for Maritime Cognitive Radio Networks. *Entropy* **2013**, *15*, 4993–5011.
13. So, J. Entropy-based Spectrum Sensing for Cognitive Radio Networks in the Presence of an Unauthorized Signal. *KSII Trans. Internet Inf. Syst.* **2015**, *9*, 20–33.

14. Peh, E.; Liang, Y.C. Optimization for Cooperative Sensing in Cognitive Radio Networks. In Proceedings of the International Conference on Wireless Communications, Networking and Mobile Computing (WiCOM) (Formerly WCNM), Shanghai, China, 21–25 September 2007; pp. 27–32.
15. Ghasemi, A.; Sousa, E.S. Collaborative spectrum sensing for opportunistic access in fading environments. In Proceedings of the First IEEE International Symposium on New Frontiers in Dynamic Spectrum Access Networks, Baltimore, MD, USA, 8–11 November 2005; Volume 27, pp. 131–136.
16. Varshney, P.R. *Distributed Detection and Data Fusion*; Springer: New York, NY, USA, 1996.
17. Jaitawat, A.; Karmakar, P. Comparison of Different Weight Assignment Strategy in Weighted Cooperative Spectrum Sensing. In Proceedings of the 7th International Conference on Computational Intelligence, Communication Systems and Networks (CICSyN), Riga, Latvia, 3–5 June 2015; pp. 53–58.
18. Bao, Z.; Ni, D.; Zhang, S. Weighted reliability cooperative spectrum sensing algorithm. In Proceedings of the 24th Wireless and Optical Communication Conference (WOCC), Taipei, Taiwan, 23–24 October 2015; pp. 5–8.
19. Shannon, C.E. A mathematical theory of communication. *Bell Syst. Tech. J.* **1948**, *27*, 379–423.
20. Pan, Z.; Wu, Y.Q. Method of thresholding using two-dimensional exponent entropy and its fast algorithm. *Comput. Appl.* **2007**, *27*, 982–985.